Enhanced liquid atomization: From flow-focusing to flow-blurring

Alfonso M. Gañán-Calvo[a)]
Escuela Superior de Ingenieros, Universidad de Sevilla, Avenida de los Descubrimientos, s/n, 41092 Sevilla, Spain

(Received 18 November 2004; accepted 20 April 2005; published online 16 May 2005)

This letter describes the generation of small turbulence scales in connection with a singular back-flow pattern leading to efficient atomization. A simple pneumatic atomizer configuration results, with a tenfold efficiency increase over available plain-jet air-blast atomizers. Back-flow atomization derives from a global bifurcation of the liquid-gas flow pattern; the bifurcation is triggered by a single geometrical parameter of the atomizer. The extremely simple geometry involved can be implemented down to the micrometric scale, thus opening the door to the improvement of current atomizers and to unprecedented designs. © *2005 American Institute of Physics*. [DOI: 10.1063/1.1931057]

Liquid atomization involves the conversion of a small part of an energy input into surface energy. The energy source is either mechanical, electromechanical, or purely electrostatic. Unfortunately, most of the source energy is dissipated, so that the atomization efficiency (surface energy/source energy) is always small, conspicuously so in the case of pneumatic atomization. The mechanical energy conveyor in pneumatic atomizers is a gas stream interacting with the liquid stream. The interaction involves several fluidic mechanisms leading to generally small droplet sizes (e.g., Ref. 1 and references therein). Atomization is obtained at the cost of a very high dissipation, owing to the presence of the gas phase in turbulent motion: An extremely low-energy efficiency is observed.

The fluidic mechanisms involved combine complex turbulent motions with deformable free surfaces and directional inhomogeneity of the multiphase flow. Human ingenuity has explored since ancient times a variety of geometries aimed at controlling the gas-liquid interaction so as to obtain a liquid aerosol. In general terms, an optimal efficiency is achieved under: (i) maximized surface production, (ii) minimized droplet coalescence, and (iii) minimized gas expense. The enormous variety of available pneumatic atomizer geometries poses a serious challenge to any attempt at classifying the devices on the basis of the fundamental underlying physical mechanism of liquid atomization. As a general rule, the efficiency of a good atomizer is roughly proportional to its complexity; in other words, efficiency is currently paid at the expense of device complexity and size.

In this work, we report the discovery of a general, simple, reproducible, and robust flow pattern which, in spite of its simplicity, gives rise to a gas-liquid interaction yielding a high efficiency. Indeed, the flow geometry here described surpasses the efficiency of "prefilming air-blast atomizers," a highly efficient albeit complex and costly technological variety. This achievement is due to the unexpected emergence of a back-flow pattern leading to small-scale perturbations. The bifurcation separating the back-flow regime from a conventional flow-focusing pattern is triggered by a single fundamental geometrical parameter $\psi = H/D$ (see Fig. 1). When ψ is decreased to about 0.25, a radical modification in the flow configuration is observed. Assuming a specific value of the liquid flow rate and the total energy input, our flow configuration will be shown to create about five to fifty times more surface than any other pneumatic atomizer of the "plain-jet airblast" type.[2]

Our proposed configuration is characterized by a liquid feed tube whose inner diameter is equal to the exit orifice diameter D. The outlet of the feed tube has the same diameter D as the exit orifice; both sections face each other, at an offset distance H. The end of the tube is sharp cut perpendicularly to its axis (see Fig. 1). Thus, the gap between the tube end and the exit orifice gives rise to a lateral cylindrical passageway (LCP). It is worth noting that the LCP surface equals the exit orifice area when $\psi = H/D = 0.25$. Consequently, when both a liquid mass flow $\dot{m}_l$ is forced through the tube and a gas mass flow $\dot{m}_g$ is forced through the LCP, a spray combining both phases is formed and leaves the device through the orifice exit. Let $\mathrm{GLR} = \dot{m}_g/\dot{m}_l$ be defined as the *gas-to-liquid mass ratio*.

In order to minimize gas friction losses between the tube walls and the exit orifice walls when ψ is small, the tube end is sharpened as sketched in Fig. 1. Experimentation has shown that our results do not depend of the border edge angle provided the angle lies (approximately) below 60°.

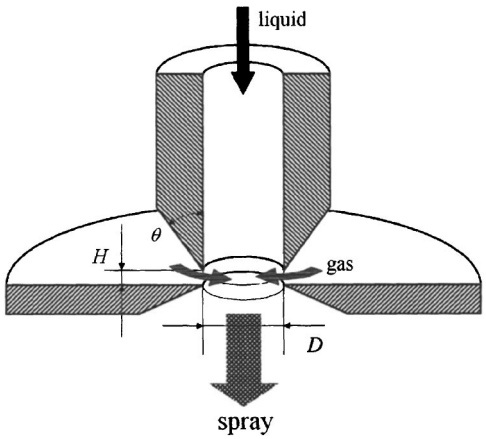

FIG. 1. Schematics of the simple nozzle geometry used. Sketch of the liquid feed orifice with diameter D aligned with an exit orifice with equal diameter D; both orifices are axially offset at a distance H.

[a)]Electronic mail: alfonso@eurus2.us.es

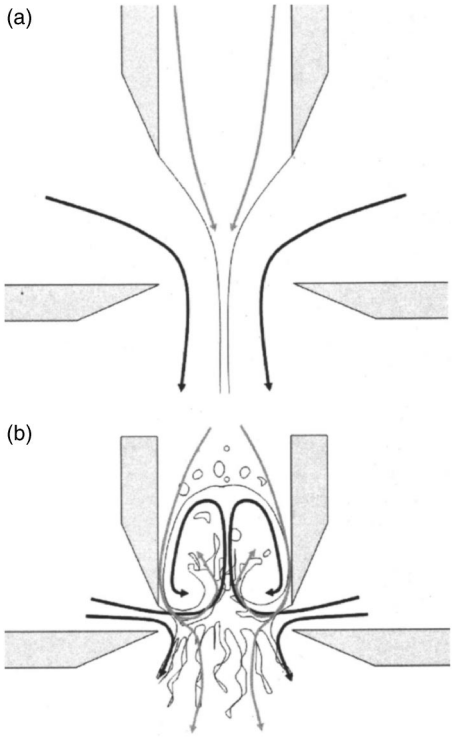

FIG. 2. (a) The FF configuration (here, $\psi=1$). (b) The FB configuration (here, $\psi=0.2$), with a back-flow mixing region at the tube mouth.

When $\psi>0.25$, the liquid flow follows the well known "flow focusing" pattern[3] [see Fig. 2(a)], with the formation of a liquid microjet. At the exit, the liquid microjet may either break up axisymmetrically to produce a quasi-monodisperse spray, or display a nonaxisymmetric or turbulent pattern leading to a polydisperse spray: the breakup mode depends on the Weber number.[3,4] We will concentrate here on high Weber number pneumatic atomization, since it ensures the best compromise between large liquid flow rate and small droplet size.

When ψ drops below 0.25, the flow pattern at the mouth of the feed tube experiences a drastic bifurcation. The gas flow becomes significantly radial, perpendicular to the symmetry axis, and a stagnation point develops between the feed mouth and the exit orifice. Thus, part of the gas flows upstream into the liquid tube and mixes turbulently with the incoming liquid [see Fig. 2(b)]. Consequently, very small scale motions governed by the well known turbulent inertial cascade mechanism[5] are produced at the tube exit region. The size distribution of this turbulent small scale is dictated by the macroscopic length scale given by the inner tube diameter, the gas overpressure, the liquid surface tension, and the liquid viscosity.[5,6] For small enough liquid viscosity (the case explored in this work), the influence of viscosity becomes negligible. As a global result, the flow self-organizes spontaneously as a function of a single geometrical parameter, providing an extremely effective means for micromixing without passive or active forcing elements. To illustrate this intriguing phenomenon, we used a glass feed tube, and a high-speed photograph of the mixing region was taken while the device was producing a fine aerosol: In Fig. 3 the turbulent structure with the production of small scales.

Thus, the resulting back-flow pattern and pre-mixing mechanism gives rise to a dramatic change in the spray plume generated. Lower velocity and wider angle are observed [see Fig. 3(c) showing a high-speed photograph of the spray as it exists the orifice]. The liquid jet has vanished; in its place, a plume consisting of unsteady chaotic liquid ligaments issues from the mixing zone. In contrast with flow focusing, we have chosen to refer to this flow pattern as "flow blurring" (FB).

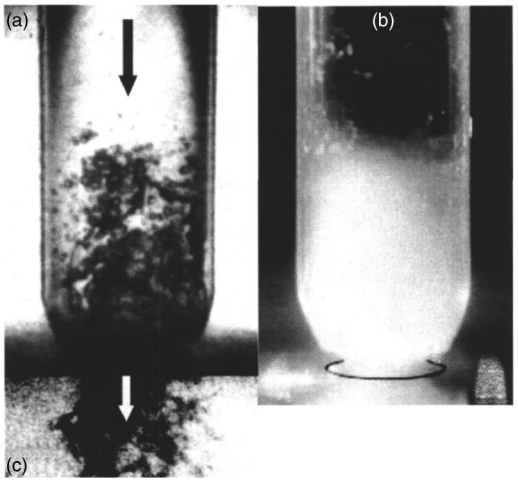

FIG. 3. Mixing region inside the tube in the vicinity of the tube exit, $D=900$ μm, $H=65$ μm, $\Delta P=76$ kPa, $Q=20$ ml/min. Tube: Borosilicate glass, inner diameter: 0.9 mm, outer diameter: 1.3 mm. Liquid: Water at 25 °C; gas: Air. (a) High speed photograph (exp. time: 100 ns); (b) Standard photograph (exposure time: 1/4 s.). (c) Spray as it exits the orifice (exp. time: 100 ns). Arrows indicate the flow direction.

Two liquids have been used in our study: Water ($\rho=997$ kg/m^3, $\sigma=73$ mN/m, $\mu=1.1$ cP, at 23 °C) and ethanol ($\rho=804$ kg/m^3, $\sigma=23$ mN/m, $\mu=1.2$ cP, at 22.6 °C), ρ, μ, and σ being the liquid density, viscosity, and surface tension. We have used air, nitrogen, and argon as co-flowing gases. Experiments have been performed at lab ambient temperature (22–23 °C). Maximum gas pressure used in this study has been 500 kPa. Droplet measurements have been carried out by the laser-diffraction technique using a Sympatec Helos BF/Magic instrument, with a R2 optics (droplet size range from 0.45 to 87.5 μm). The distance from the nozzle exit to the measurement point is set at the minimum value where the effects of droplet coalescence and turbulent breakup become negligible ("relaxation" length).[7] This distance is experimentally determined as a function of the droplet size for each nozzle orifice diameter. Nevertheless, in our measurements, it is worth noting that the droplet size is almost determined, within a range of at most ±20%, by the initial droplet size as produced at the nozzle exit. Two dimensionless numbers (as described by Refs. 2, 6, and 8) are introduced:

$$We_D=\rho_g U_g^2 D(2\sigma)^{-1}, \quad Oh_D=\mu(\rho_l\sigma D)^{-1/2}, \tag{1}$$

where ρ_g and U_g are the density and gas velocity: (i) at the exit orifice when $\psi>0.25$ (the liquid cross section is assumed negligible compared to the orifice section) or (ii) at the LCP when $\psi<0.25$. The values of ρ_g and U_g, as well as the pressure drop across the orifice are univocally determined by the gas mass flow rate $\dot{m}_g$; to that end and in the absence of a better postulate, the gas is assumed to expand adiabatically from the source to the external ambient, either through the exit orifice or the LCP. The dimensionless droplet mass median diameter (MMD) is defined as $\delta=\mathrm{MMD}/D$. The geometrical standard deviation ranged from 1.8 to 2.1 in all

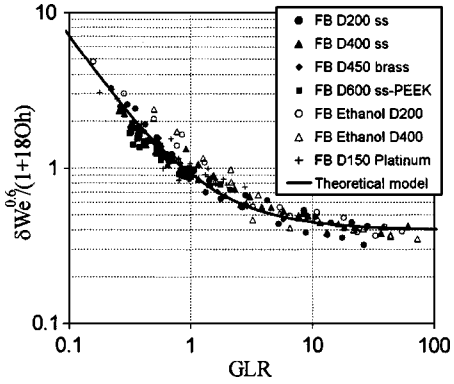

FIG. 4. Data plot of $\delta We_D^{0.6}(1+18Oh_D)^{-1}$ versus GLR, for FB experiments using several orifice diameters, with water and ethanol. The label identifies each experimental series by referring to its orifice diameter (D600 implies a 600 μm diameter) and the materials in the device (ss is stainless-steel AISI 316). When different materials are used, [e.g., poly ether ether ketone (PEEK)-ss] the first one is the feeding tube material, and the second is the orifice plate material. Unless otherwise specified (e.g., ethanol), the liquid used is distilled water at 23 °C. Plot of the model function is also shown.

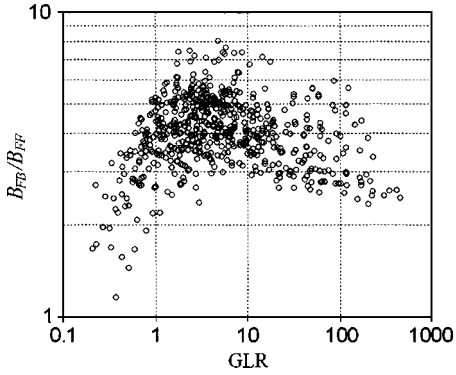

FIG. 5. Data plot for the efficiency gain of FB over FF in experiments using several orifice diameters, with water and ethanol.

our measurements, showing a negligible dependence on the liquid properties and working parameters as long as the devices were operated in the FB regime. As a result, the following dimensionless expression is formally derived; it determines the final droplet diameter distribution, assuming a fully mixed and relaxed state (e.g., Ref. 9)

$$\delta = \delta(\psi, We_D, Oh_D, \mathrm{GLR}). \tag{2}$$

At this point, in order to get a close predictive model for δ, inspiration may be drawn from the classical approach of Shinnar[10] (followed by many authors, e.g., Ref. 6 and references therein), which is solidly supported by the classical Kolmogorov–Hinze theory on the observation of the mixing region from which the spray emanates. A further dependence on the GLR and on Oh_D, as suggested by many works and adapted to the present configuration, can be included in the following form (e.g., Ref. 6 and references therein):

$$\delta = C_1 We_D^{-0.6}(1 + C_2 Oh_D)(1 + C_3 \mathrm{GLR}^{-1})^{1.2}, \tag{3}$$

where a linear dependence on Oh_D is considered as a first approximation for $Oh_D \ll 1$.

In Fig. 4, many experimental measurements are plotted. Several orifice diameters ranging from 100 μm to 600 μm and different nebulizer materials are used; the liquid is chosen to be water or ethanol. The best fit within experimental uncertainty is reduced to $C_1 = 0.42$, $C_2 = 18$, and $C_3 = 1$. A good data collapse is observed in Fig. 4, providing confidence in our chosen theoretical model.

An interesting issue concerning the data collapse in Fig. 4 is the fact that water and ethanol, whose droplets exhibit a very different tendency to coalesce, seem to follow here the same droplet size prediction in spite of this difference. This is consistent with the immediate scattering of the spray [evidenced in Fig. 3(b)], which inhibits the important early coalescence effects of other atomizer configurations. Evident analogies concerning explosive spray divergence can be observed between our Figs. 3(b) and Fig. 2(b) in Hopfinger and Lasheras.[9]

Finally, since the atomizer efficiency can be expressed as:

$$B = (6\sigma Q_l)\mathrm{SMD}^{-1}(Q_l \Delta P + \dot{m}_g \Delta h_o)^{-1}, \tag{4}$$

where Δh_o and ΔP are the total enthalpy drop and pressure drop across the orifice, the efficiency gain of FB over FF is given by the inverse of the droplet Sauter mean diameter (SMD) ratio measured for both configurations, all parameters being identical except ψ:

$$\frac{B_{\mathrm{FB}}}{B_{\mathrm{FF}}} = \frac{\mathrm{SMD}_{\mathrm{FF}}}{\mathrm{SMD}_{\mathrm{FB}}}. \tag{5}$$

Figure 5 plots the efficiency gain $B_{\mathrm{FB}}/B_{\mathrm{FF}}$ for a set of experiments involving several orifice diameters and using water and ethanol. As can be gathered from the plot, a dramatic increase in the atomizer efficiency is experienced when using the FB topology.

In summary, a new flow regime (flow blurring or backflow mixing) is here described, with unexpected features making it suitable for low-energy microturbulent generation. We have been able to increase the efficiency of pneumatic atomization up to an order of magnitude above any other existing co-flowing or plain-jet air-blast geometries.

The author is grateful for financial support from the Ministry of Science and Technology of Spain, Grant No. DPI2002-04305-C02-02. Fruitful discussions with Dr. Joan Rosell and Dr. Riesco-Chueca are greatly appreciated. The assistance of Eladio Mendoza, Jorge López, Manuel Martín, and Braulio Gañán-Riesco in the experiments is also greatly appreciated.

[1] Y. Zimmels and S. Sadik, Appl. Phys. Lett. **79**, 4601 (2001).
[2] A. H. Lefebvre, *Atomization and Sprays* (Hemisphere, New York, 1989).
[3] A. M. Gañán-Calvo, Phys. Rev. Lett. **80**, 285 (1998).
[4] J. M. Gordillo, M. Pérez-Saborid, and A. M. Gañán-Calvo, J. Fluid Mech. **448**, 23 (2001).
[5] H. Tennekes and J. L. Lumley, *A First Course in Turbulence* (MIT Press, Cambridge, MA, 1972).
[6] T. Lemenad, D. D. Valle, Y. Zellouf, and H. Peerhossaini, Int. J. Multiphase Flow **29**, 813 (2003).
[7] J. C. Lasheras and E. C. Hopfinger, Annu. Rev. Fluid Mech. **32**, 275 (2000).
[8] D. A. Nguyen and M. J. Rhodes, Powder Technol. **99**, 285 (1998).
[9] E. C. Hopfinger and J. C. Lasheras, Phys. Fluids **8**, 1696 (1996).
[10] R. Shinnar, J. Fluid Mech. **10**, 259 (1961).